

IUE OBSERVATIONS OF RW HYDRAE (gM2 + pec)

M. KAFATOS¹

Department of Physics, George Mason University

AND

A. G. MICHALITSIANOS AND R. W. HOBBS

Laboratory for Astronomy and Solar Physics, NASA Goddard Space Flight Center

Received 1979 December 3; accepted 1980 February 28

ABSTRACT

IUE observations of the late type star RW Hya (gM2 + pec) have been obtained. Analysis of the intense UV continuum observed between 1100 and 2000 Å suggests that this object is a binary system in which the secondary is identified as the central star of a planetary nebula with $T_{\text{eff}} \sim 10^5$ K. The ultraviolet spectrum is characterized by semiforbidden and allowed transition lines, of which the C IV (1548 Å, 1550 Å) doublet is particularly strong. A general absence of strong forbidden line emission suggests that the compact nebula in which both primary and secondary stars are embedded has particularly high densities of $\sim 10^8$ – 10^9 cm⁻³. Tidal interaction rather than steady state mass flow from the M giant is suggested as a means to form a nebula with the characteristic densities inferred from our UV line analysis. RW Hya is suggested as a possible source of soft X-ray emission if material is accreting onto the surface of the secondary. A general discussion concerning the ionic abundances of various atomic ions present is given.

Subject headings: nebulae: planetary — stars: binaries — stars: combination spectra — stars: individual — stars: long-period variables — ultraviolet: spectra

I. INTRODUCTION

Far-ultraviolet observations obtained with the *International Ultraviolet Explorer* (*IUE*) between 1200 and 3200 Å of the late type star RW Hya (gM2 + pec) suggests this object is a binary system. RW Hya was selected for *IUE* observations because it exhibits a composite spectrum in the visible, in which a late type spectrum typical of cool M giants has superposed permitted and forbidden emission lines, and suggests the presence of a circumstellar nebula excited by a hot subluminal star. From our data RW Hya appears to be a true symbiotic star in which the hot companion is most likely classified as a central star of a planetary nebula with $T_{\text{eff}} \sim 10^5$ K that ionizes a compact nebula. Our findings are consistent with the conclusions of Merrill (1950), who found that displacement velocities observed in optical lines support a binary star model. The highly excited gaseous envelope gives rise to very strong C IV (1548 Å, 1550 Å) that appears unusually strong and suggests a high energy source of emission.

From our UV absolute measurements of line and continuum emission we have deduced the general properties of the stars that form the RW Hya system and the ionization structure of the nebula which is excited by the hot companion. *IUE* has been particularly useful in this regard in observing late type stars with composite spectra because the emission of the

cool M giant does not overwhelm the emission of the companion in the far-ultraviolet. Details concerning our observations and analysis are given in the following sections. *IUE* instrumentation is described in detail by Boggess *et al.* (1978).

II. ULTRAVIOLET SPECTRAL OBSERVATIONS

Ultraviolet observations were obtained of RW Hya on 1979 July 29 and September 1 over the wavelength range 1200–3200 Å using exclusively the large aperture (10" × 20") of the *IUE* spectrometer. Low dispersion spectra of RW Hya taken with a limiting spectral resolution of ~ 6 Å in the short wavelength range (1100–2000 Å) on both observing dates show virtually no change in UV continuum or line emission intensity. Initial exposures of RW Hya using the short wavelength camera with 15 minute exposures revealed strong UV continuum and semiforbidden and permitted line emission. $\text{L}\alpha$ 1216 Å is observed in absorption (Fig. 1a). Echelle spectra obtained on September 1 showed essentially the same spectral structure observed previously. High dispersion (~ 0.1 Å resolution) spectra obtained on September 1 in the short wavelength range are shown for only selected features in Figures 2, 3, and 4, with all line identifications given in Table 1. Long wavelength exposures (2000–3200 Å) show intense continuum for which F_λ is independent with wavelength (Fig. 1b). Identified emission lines and absolute fluxes are shown in Table 1. The emission lines of C II] (2325 Å, 2327 Å, 2328 Å), O III (3047 Å,

¹ Work supported by NASA grant NSG 5371.

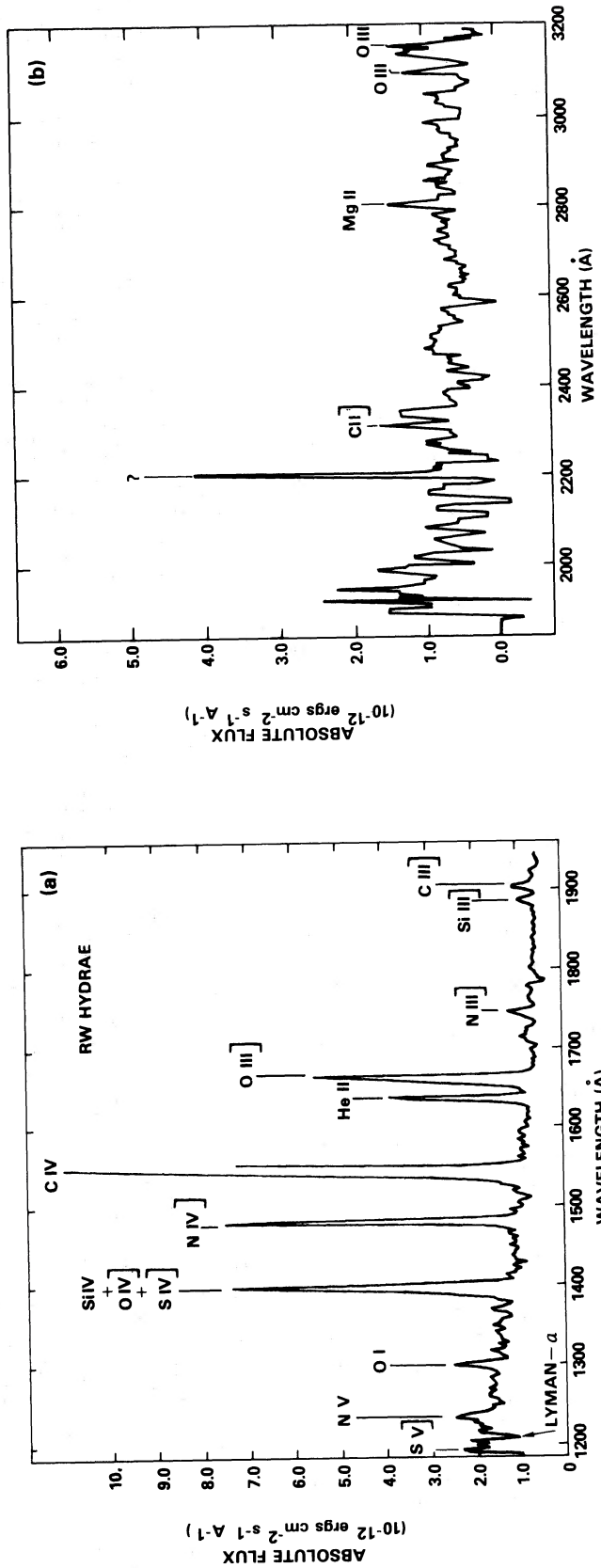


FIG. 1.—(a) Low-dispersion ($\sim 6 \text{ \AA}$ resolution) short-wavelength spectrum of RW Hya. The C IV lines (1548 Å, 1550 Å) are saturated and off scale. Ly α is in absorption and due to interstellar extinction. The continuum rises toward short wavelengths and is approximated by a blackbody continuum curve that corresponds to $T_2 = 100,000 \text{ K}$. The peak in the blackbody continuum occurs most likely below the detectable range of the *IUE* spectrometer, i.e., $\sim 500 \text{ \AA}$. (b) Low-dispersion long-wavelength spectrum of RW Hya. The spectrum is dominated by continuum that is independent with wavelength. Few strong emission lines are recorded with the exception of Mg II, C II], and O III. The spike at 2200 Å is attributed to noise. A distinct lack of forbidden emission lines is noted.

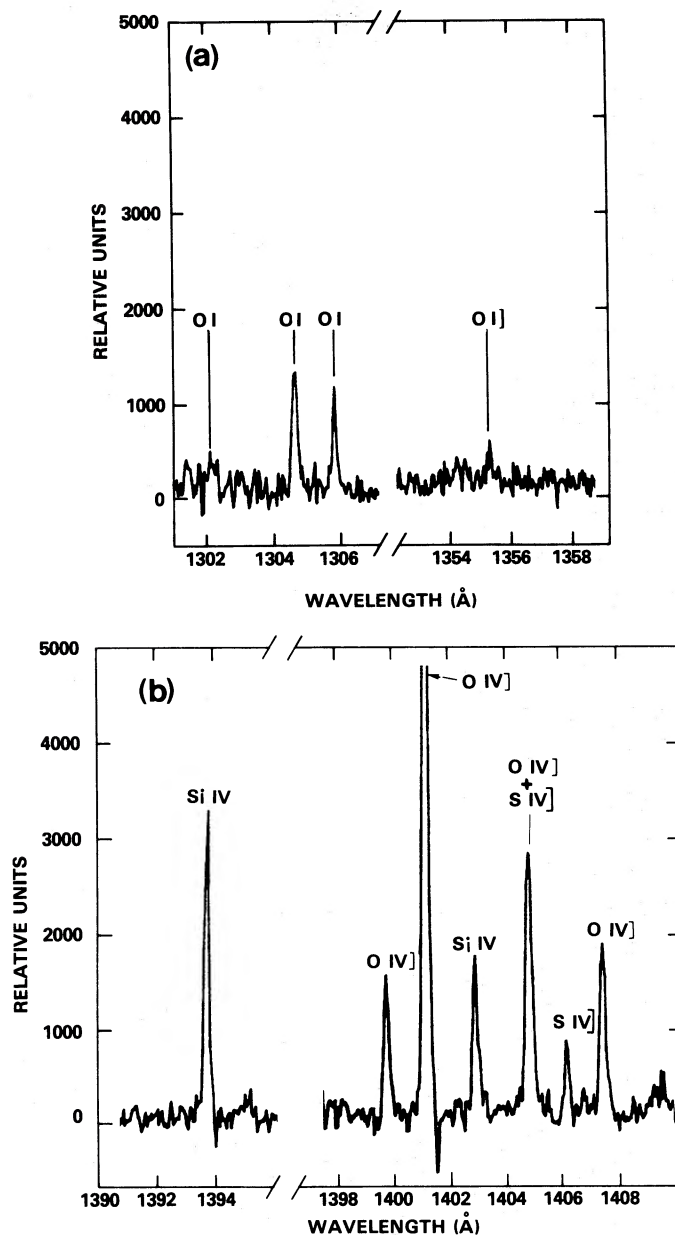


FIG. 2.—(a) High-dispersion (~ 0.1 Å resolution) showing O I lines between 1302 and 1358 Å. Intensity expressed in relative intensity units. (b) High-dispersion spectrum showing Si IV, O IV], and S IV].

3133 Å), and Mg II (2796 Å, 2803 Å) are the only lines recorded in the long wavelength range.

In Table 1, ionic transitions indicated with a question mark are doubtful identifications. Wavelengths shown in column (2) of Table 1 with question marks have ambiguous published wavelengths (Edlén 1972; Weise, Smith, and Glennon 1966). The numerous Fe II features that are questionably identified, with the exception of the (43) multiplet, are so identified because of their relatively weak emission. The general absence of strong forbidden line emission will have relevance to our analysis in §§III*d* and IV.

Also shown in Table 1 are absolute fluxes for the strongest lines identified. Absolute flux estimates were obtained from low-dispersion spectra using the data reduction routines developed for the PDP 11/40 computer at NASA Goddard by Drs. Klinglesmith and Fahey. Software does not exist at present to determine absolute line flux emission from high-dispersion spectra. Accordingly, strong emission features evident in low-dispersion spectra represent a blend of closely spaced high excitation lines; e.g., the feature at 1398.1 Å is a blend consisting of Si IV, O IV], and S IV]. The spectra obtained here were obtained after cor-

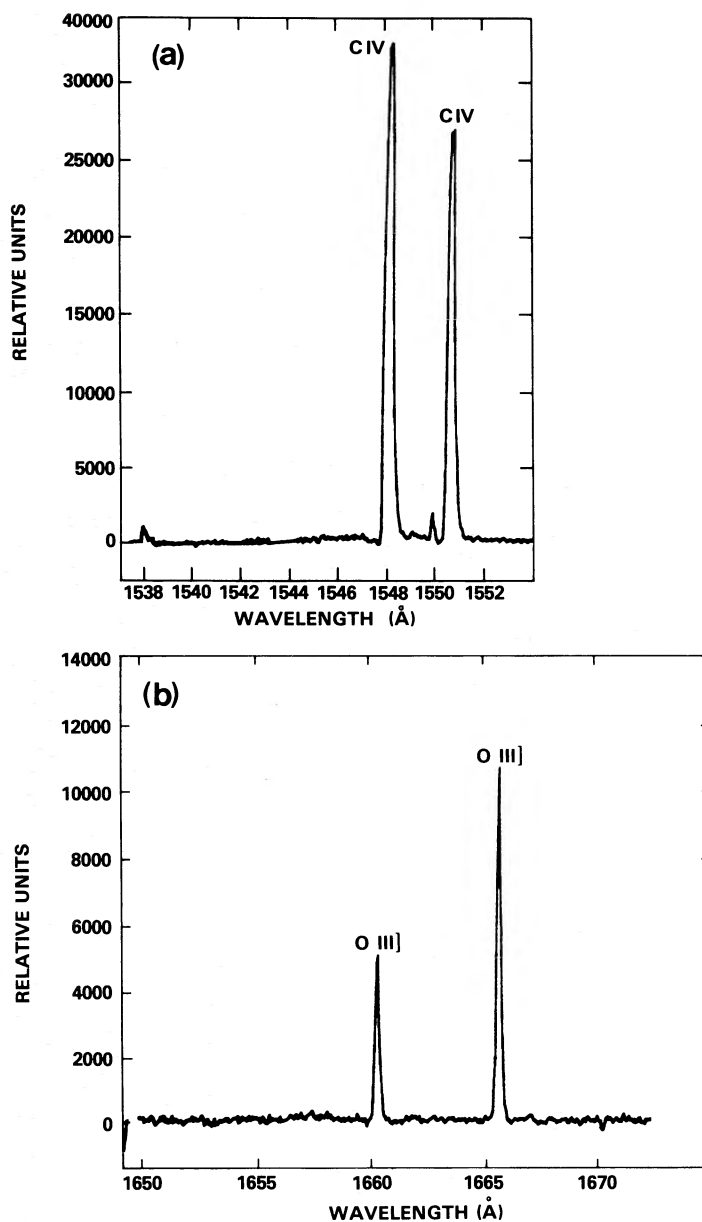


FIG. 3.—(a) High-dispersion spectrum of the C IV (1548 Å, 1550 Å) lines with Fe II at 1550.260 Å. (b) High-dispersion spectrum of the O III] lines at 1660.803 Å and 1666.153 Å.

rections to the intensity transfer function were implemented and as such are not affected by calibration errors in reduction.

III. DATA ANALYSIS OF RW HYDRAE

RW Hydrae has been a suspected symbiotic star from previous visual observations. The light cycle of the primary has been known from Yamamoto (1924) to vary with a period of approximately 370 days, which is comparable to the 376 day orbital period for the secondary determined from radial velocity observations of emission and absorption lines by Merrill

(1950). The gM2 spectrum in the visual consists of H, He I, He II, [O III], [Ne III], [Fe V], and [Fe VII] from data of Merrill and Humason (1932), Merrill (1933, 1940, 1944, 1950), and Swings and Struve (1941, 1942). The results of our UV observations and analysis are described in the following sections.

a) Distance to RW Hydrae

From equivalent width measurements of the $L\alpha$ absorption line 1216 Å we find that $W_{1216\text{Å}} \sim 1.5$ Å, and using curve-of-growth analysis appropriate for the "square root" segment of the curve of growth (Spitzer

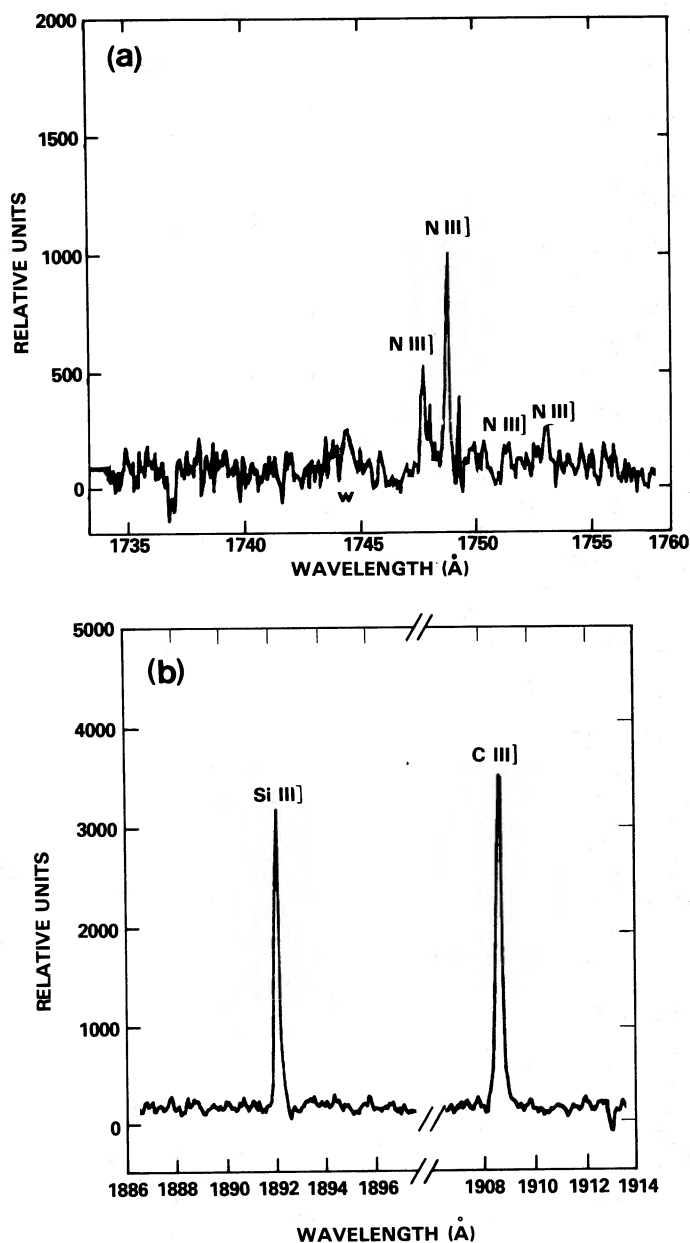


FIG. 4.—(a) High-dispersion spectrum of the N III] lines around 1750 Å. (b) High-dispersion spectrum showing Si III] and C III] at 1892.030 Å and 1908.734 Å, respectively.

1978), we obtain a column density in our line of sight $N_{\text{H I}} \sim 6.38 \times 10^{18} \text{ cm}^{-2}$. This value corresponds to a color excess $E(B - V) \sim 1.3 \times 10^{-3}$ which was obtained from the column density and $E(B - V)$ relationship for interstellar extinction of Savage and Mathis (1979). In the Rayleigh-Jeans region the blackbody curves that we have fitted incorporate values of $E(B - V)$ that correspond to the value obtained above for the distribution of continuum with wavelength observed if the star has a temperature $\geq 50,000$ K. Accordingly, since the adopted value of $E(B - V)$ is

very small, we can assume essentially no absorption in the ultraviolet.

Since the primary star is a gM2 spectral type (Merrill 1950), we can estimate the absolute magnitude of the red giant by assuming it is an M2 III star whose absolute magnitude from Allen (1973) is $M_V \sim -0.6$. Knowing the observed apparent magnitude $m_V \sim 10$ and M_V , we deduce a distance to RW Hya of $D \sim 1.3 \times 10^3$ pc. This distance corresponds to an average density in the line of sight $\bar{n}_{\text{H I}} \sim 1.6 \times 10^{-3} \text{ cm}^{-3}$ for a height above the galactic plane $Z \sim 780$ pc.

TABLE 1
LINE IDENTIFICATION AND FLUXES

Ionic Transition	Wavelength (Å)	Wavelength of <i>IUE</i> Feature (Å)	Flux (ergs cm ⁻² s ⁻¹) ^a
C III	1174.933 + 1175.263	1175.046	
C III	1175.590 + 1175.711 + 1175.987	1175.758	
C III	1176.370	1176.870	
S V ⁽¹⁾	1199.180	1199.200	1.56 × 10 ^{-12b}
Si III	1206.510	1206.604	
N V	1238.821	1238.836	
N V	1242.804	1242.816	2.73 × 10 ⁻¹¹
C III	1247.383	1247.502	
O I	1302.169	1302.468	
O I	1304.857	1304.958	1.83 × 10 ⁻¹¹
O I	1306.029	1306.132	
O I	1355.598	1355.754	
Si IV	1393.755	1393.930	
O IV	1399.774	1399.810	
O IV	1401.156	1401.198	5.08 × 10 ⁻¹¹
Si IV	1402.770	1402.928	
S IV] + O IV]	1404.770 + 1404.812	1404.770	
S IV]	1406.000	1406.084	
O IV]	1407.386	1407.414	
N IV]	1486.496	1486.512	5.59 × 10 ⁻¹¹
C IV	1548.185	1548.448	
Fe II?	1550.260	1550.244	3.89 × 10 ⁻¹⁰
C IV	1550.774	1550.972	
[Ne IV] [?] (2)	1601.500 + 1601.700(?)	1601.330	
Fe II	1625.520 (43) multiplet	1625.040	
Fe II	1632.668 (43) multiplet	1643.818	
He II	1640.332	1640.412	2.07 × 10 ⁻¹¹
Fe II?	1641.759 (68) multiplet	1641.428	
Fe II?	1643.576 (42) multiplet	1643.818	
Fe II?	1652.185 (42) multiplet	1652.186	
Fe II?	1654.446 (42) multiplet	1654.476	
Fe II?	1655.042 (68) multiplet	1655.774	
O III]	1660.803	1660.914	4.10 × 10 ⁻¹¹
O III]	1666.153	1666.248	
N III]	1748.610	1748.840	
N III]	1749.674	1749.794	8.27 × 10 ⁻¹²
N III]	1752.160	1752.378	
N III]	1753.986	1754.164	
[Ne III] [?] (3)	1793.800?	1795.616	
Si II	1808.012	1808.370	
Si II	1816.928 + 1817.451	1817.000	
Al III	1854.716	1854.946	
Al III	1862.790	1863.000	
Si III]	1892.030	1892.172	4.27 × 10 ⁻¹²
C III]	1908.734	1908.922	5.76 × 10 ⁻¹¹
C II] + [O III] [?] (4)	2325 + 2327 + 2328 + 2321.7?	2332.400	2.43 × 10 ⁻¹¹
[Ne IV] [?] (5)	2422.500 + 2425.100?	2432.600	
[O II] [?] (6)	2471.100?	2486.800	
Mg II	2796 + 2803	2799.400	1.00 × 10 ⁻¹¹
O III	3047	3040.000	9.70 × 10 ⁻¹²
O III	3133	3141.600	2.62 × 10 ⁻¹¹

^a Absolute fluxes obtained from low dispersion spectra (~6 Å spectral resolution).

^b S V] 1196.8 Å absolute flux is questionable because *IUE* sensitivity is dropping rapidly at this wavelength.

NOTE.—All wavelengths shorter than 2000 Å are from Kelly and Palumbo (1973) unless otherwise noted. Short-wavelength spectra are obtained in high dispersion (~0.1 Å resolution).

⁽¹⁾ Wavelengths from Cohen, Feldman, and Doschek 1978.

⁽²⁾ Wavelengths from Edlen 1972 (E). This disagrees with the wavelengths published by Wiese, Smith, and Glennon 1966 (WSG), who give the two wavelengths as 1608.8 Å and 1609.0 Å, respectively.

⁽³⁾ Wavelength from E agrees with WSG. Published wavelength, however, may be wrong because it is subject to large uncertainties.

⁽⁴⁾ [O III] wavelength from E and WSG give 2326.35 Å.

⁽⁵⁾ Wavelengths from E and WSG give them as 2438.5 Å and 2441.3 Å, respectively.

⁽⁶⁾ Wavelength from E; WSG give it as 2470.4 Å.

We doubt that M_V could be much less than -0.6 because the height above the galactic plane would be correspondingly greater and $\bar{n}_{\text{H I}}$ would be even smaller. On the other hand, M_V could be larger since, according to Plaut (1965), M_V can be as large as zero for long period variables. Using $M_V = 0.0$, a distance $D \sim 10^3$ pc is found for which $\bar{n}_{\text{H I}} \sim 2.1 \times 10^{-3} \text{ cm}^{-3}$ and $Z \sim 600$ pc. The corresponding stellar parameters would then be $M_{\text{bol}} \sim -2.2$, $\log L_*/L \sim 2.78$, and $\log R_*/R \sim 1.92$. According to Bohlin (1975) a column density $N_{\text{H I}} < 10^{19} \text{ cm}^{-2}$, and density $\bar{n}_{\text{H I}} < 0.03 \text{ cm}^{-3}$ for the early type star α Vir ($l'' = 316^\circ$, $b'' = +51^\circ$) has been found, that is, a star which lies in a region of the same approximate galactic coordinates as RW Hya. Therefore, the values of $N_{\text{H I}}$ and $\bar{n}_{\text{H I}}$ obtained here for RW Hya are not inconsistent with the values obtained by Bohlin for a star that is at least in a similar part of the sky. Moreover, the height found for RW Hya above the galactic plane is consistent with the distribution of red giants and long period variables found by Blaauw (1965). Since the parameters obtained for the two absolute magnitudes assumed here are similar, we will adopt the values $M_V = 0.0$ and $D = 10^3$ pc in our analysis. In Table 2 the properties of the red giant primary and the hot secondary are denoted by subscripts 1 and 2, respectively.

b) Properties of the Secondary

The UV continuum flux between 1200 and 1900 Å is best approximated by a Rayleigh-Jeans blackbody curve for temperatures $T_{\text{eff}} \gtrsim 50,000$ K that is further consistent with the strong He II 1640 Å emission observed. We attribute the continuum to thermal emission from the hot companion. As such, from the observed flux at 1300 Å of $F_\lambda \sim 1.5 \times 10^{-12} \text{ ergs cm}^{-2} \text{ s}^{-1} \text{ Å}^{-1}$, we obtain an apparent visual magnitude for the companion $m_V \sim 14.75$. In contrast to the apparent magnitude of the primary, $m_V \sim 10$, the secondary companion would not be observable in the visual because the primary dominates the integrated light. However, by virtue of the high temperature of the companion it dominates the UV.

An upper temperature limit can be obtained by requiring that the luminosity be less than the Edding-

ton luminosity (for $1 M_\odot$). Accordingly, we estimate that the temperature can not exceed $T_2 = 200,000$ K. As seen in Table 2, we have calculated parameters for the companion at 1000 pc for three different models: (1) $T_2 = 50,000$ K, (2) $T_2 = 100,000$ K, and (3) $T_2 = 200,000$ K. In Figure 5 the corresponding locations of the primary and secondary are shown on the H-R diagram. We note that the location of the secondary in the figure falls well within the region occupied by central stars of planetary nebulae. We conclude the temperature for the secondary is in the range $5 \times 10^4 \leq T_2 \leq 2 \times 10^5$ K. The primary is located in the region occupied by long period variables (LPV, from Allen 1973). The Wolf-Rayet and central stars of planetary nebulae are from Osterbrock (1974). For the best estimated temperature of the secondary $T_2 = 100,000$ K (see § IIIc) the primary and secondary have about equal luminosities.

c) Properties of the Excited Nebula

Between 2000 Å and 3200 Å the continuum contribution of the companion is assumed negligible in comparison to the nebular continuum. As such, the continuum in this spectral range is attributed to Balmer recombination emission for reasons that will be made evident further in the text. At ~ 2400 Å the measured continuum flux is $F_\lambda \sim 5 \times 10^{-13} \text{ ergs cm}^{-2} \text{ s}^{-1} \text{ Å}^{-1}$ (Fig. 1b), and yields a relation for continuum emission for an ionized nebula which is

$$n_e^2(L/L_0)^3 D_{1000}^{-2} \sim 3.45 \times 10^{18} \text{ cm}^{-6} \quad (1)$$

(see Osterbrock 1974) that is valid for $10^4 \leq T_e \leq 2.5 \times 10^4$ K, where n_e is the electron density of the nebula and L is the linear size of the nebula scaled with respect to the semimajor axis a_0 of the secondary's elliptical orbit, i.e., $L_0 \equiv 2a_0$. The distance D is scaled in units $D_{1000} = D/1000$ pc. Equation (1) was deduced assuming the masses of the primary and secondary are in the ratio $M_1/M_2 \sim 2$ if $M_2 \sim 1 M_\odot$, which corresponds to $a_0 = 2.2 \times 10^{13} \text{ cm}$ ($L_0 = 4.4 \times 10^{13} \text{ cm}$) for an assumed orbital period ~ 376 days (Merrill 1950).

From the Strömgen relation we have

$$n_e^2(L/L_0)^3 \sim 1.26 \times 10^{19} N_{47} \text{ cm}^{-6} \quad (2)$$

TABLE 2
STELLAR PARAMETERS ($D = 1000$ pc)

PARAMETER	PRIMARY	SECONDARY		
		Model 1	Model 2	Model 3
Absolute magnitude M_V	0.0 (assumed)	4.78	4.78	4.78
Temperature (K)	3100	50,000	100,000	200,000
Bolometric magnitude M_{bol}	-2.2	-0.28	-3.00	-5.86
Luminosity $\log L_*/L_\odot$	2.78	2.01	3.10	4.25
Radius $\log R_*/R_\odot$	1.92	-0.87	-0.92	-0.95
Surface gravity $\log g_*$ (cgs)	0.91	6.17	6.28	6.30
Number of ionizing photons N_i (s^{-1}).....	7.55×10^{45}	9.18×10^{46}	8.37×10^{47}	

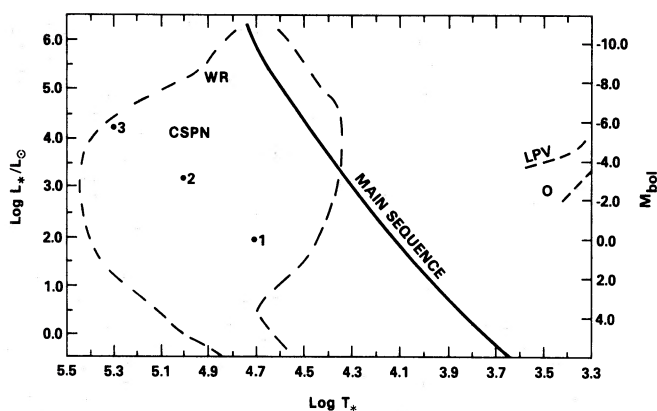


FIG. 5.—H-R diagram for the two stars in the RW Hya system. *Open circle*, primary. *Full circle*, secondary. Three secondary models are shown: 1, 2, 3 for $T_2 = 50,000$ K, $T_2 = 100,000$ K, and $T_2 = 200,000$ K, respectively. WR: Wolf-Rayet stars. CSPN: central stars of planetary nebulae. LPV: long period variables.

(see Spitzer 1978), where $N_{47} = N_i/10^{47} \text{ s}^{-1}$. Accordingly, for equations (1) and (2) to be in close agreement at a distance $D_{1000} = 1$, we require $N_{47} \sim 0.27$. From Table 2 this constrains T_2 to be in the range $5 \times 10^4 \leq T_2 \leq 10^5$ K.

The results of Hummer and Mihalas (1970) indicate that the effective stellar temperatures near our lower estimated range of $T_2 \sim 50,000$ K do not supply enough ionizing photons to explain the observed line emission. At $T_2 \sim 10^5$ K the overall number of ionizing photons N_i predicted by the models of Hummer and Mihalas (1970) is not greatly different from the estimated number of photons that arise from a blackbody. Therefore, it seems likely that the secondary has a temperature $T_2 \sim 10^5$ K.

d) Analysis of UV Emission Lines

As has been seen in Table 1, the UV spectrum of RW Hya is dominated by allowed and semiforbidden lines, with the primary emission arising from spectral lines of ions with ionization potentials ≥ 30 eV. We consider here emission from allowed and semiforbidden lines which will be followed by a discussion concerning the forbidden lines and low ionization allowed lines of O I, Si II, Mg II, and Fe II.

From the observed line strengths of allowed lines we can estimate the chemical abundances of the elements involved and the relative ionic abundances. Since for the semiforbidden lines the spontaneous transition probabilities A_{21} are $\sim 100 \text{ s}^{-1}$, this yields $n_e q_{21}/A_{21} \lesssim 1$, for densities $\lesssim 10^9 \text{ cm}^{-3}$, where q_{21} is the de-excitation rate for semiforbidden transitions (Osterbrock 1974). This statement, of course, is true for allowed lines as well. The line strengths, therefore, are proportional to $n_e^2 L^3$. The line strengths are also sensitive to the electron temperature T_e of the nebula, where we have used the value of $n_e^2 L^3$ from equation (1). The relevant atomic data for these particular UV lines was found from the following references: He II, C II], N III], N V, O III], O IV], Si II, S IV], and S V] from Osterbrock (1963); C III], C IV, Si III], Si IV, Mg II from

Osterbrock (1974); N IV] from Osterbrock (1970); and forbidden lines from Kafatos and Lynch (1980).

In Table 3 we give the abundances of the elements C, N, O, Si, and S as deduced from the UV lines for three different nebular temperatures: 10,000 K, 12,500 K, and 15,000 K. We also show the cosmic abundances from Cameron (1973) in Table 3 for comparison. We see that for $T_e = 10,000$ K, N, O, and S are much less abundant as compared to their respective cosmic abundances; for $T_e = 15,000$ K, C and Si are much less abundant, while N, O, and S are considerably more abundant than their respective cosmic abundances. An intermediate case, say $T_e \sim 12,500$ K, is therefore more reasonable. For this temperature N, O, and S are within a factor ~ 2 of their respective cosmic abundances, while C and Si are underabundant by a factor ~ 5 and ~ 7 , respectively. For the nebular temperatures considered, the chemical abundances deduced are model sensitive and vary by more than an order of magnitude for temperatures $T_e = 10,000$ K and $T_e = 15,000$ K. It is not clear whether the depletion of C and Si in this case might be due to the formation of grains or silicates, or to stellar evolution effects. In Table 3 we also show the relative ionic abundances. Some N II, Si V, S II, and S III may also be present where the ionic abundances of N, Si, and S ions are upper limits (but not expected to be too different from the values given in the Table). It is curious that the forbidden line of O II at 2471 Å is very weak. Since Al III is present (Al III having a lower ionization potential than O II), the weakness of the [O II] line is probably due to high densities. For $n_e \sim 10^9 \text{ cm}^{-3}$ and for an estimated upper limit of the [O II] flux of $\sim 2 \times 10^{-12} \text{ ergs cm}^{-2} \text{ s}^{-1}$, we deduce that the relative ionic abundance of O II is less than 0.19 (for lower densities it is correspondingly lower). The O III and O IV abundances are more than 0.569 and 0.281, respectively. These abundances are shown in the parentheses.

The nebular parameters can also be obtained from an analysis involving the C III lines. We estimate

TABLE 3
A. NEBULAR PARAMETERS

Element Abundance	$T_e = 10,000$ K	$T_e = 12,500$ K	$T_e = 15,000$ K	Cosmic Abundance
C.....	3.71×10^{-4}	7.09×10^{-5}	2.42×10^{-5}	3.71×10^{-4}
N.....	10^{-5}	7.59×10^{-5}	2.83×10^{-4}	1.18×10^{-4}
O.....	1.60×10^{-4}	9.16×10^{-4}	2.84×10^{-3}	6.76×10^{-4}
Si.....	3.14×10^{-5}	4.21×10^{-6}	1.22×10^{-6}	3.14×10^{-5}
S.....	7.62×10^{-7}	6.82×10^{-6}	2.85×10^{-5}	1.57×10^{-5}

B. $T_e = 12,500$ K MODEL

Ion	Relative Ionic Abundance
C II.....	0.074
C III.....	0.143
C IV.....	0.783
N III.....	0.077
N IV.....	0.373
N V.....	0.550
O II.....	... (<0.190) ^a
O III.....	0.654 (>0.529)
O IV.....	0.346 (>0.281)
Si III.....	0.113
Si IV.....	0.887
S IV.....	0.319
S V.....	0.681
He III.....	0.02

^a From upper limit to the [O II] line flux.

$I(1909 \text{ \AA})/I(1176 \text{ \AA}) \geq 15$, and from Louergue and Nussbaumer (1974) we find that $n_e \lesssim 10^9 \text{ cm}^{-3}$ for $T_e \lesssim 20,000$ K. Moreover, we estimate that $I(1174.93 \text{ \AA} + 1175.26 \text{ \AA})/I(1176.38 \text{ \AA}) \sim 1$, and $I(1175.59 \text{ \AA} + 1175.71 \text{ \AA} + 1175.99 \text{ \AA})/I(1176.38 \text{ \AA}) \sim 1$, and from Louergue and Nussbaumer (1976) we find that $n_e \lesssim 10^9 \text{ cm}^{-3}$ and $T_e \lesssim 20,000$ K. These estimates are in agreement with our previous analysis of strong UV allowed and semiforbidden emission lines.

The He II 1640 Å was also detected. Since it is a recombination line (of He III), it is weakly dependent on T_e . For the value $n_e^2 L^3$ which we have been using and from the cosmic abundances we find that the ionic abundance of He III is ~ 0.02 . This particularly low abundance of He III is in conflict with the abundances of N IV, O III, and S V shown in the table. Since all of the line fluxes are proportional to $n_e^2 L^3$, this result cannot be due to density arguments. Additionally, the low abundance of He III is found for all temperatures that we have considered. We doubt that chemical abundance arguments can resolve this conflict since helium would have to be underabundant by a factor ~ 10 . At present we cannot comprehend this low value.

The O I, Si II, Mg II, and the possible Fe II lines may be originating from regions different from the compact nebula. This follows since, using the value of $n_e^2 L^3$ from equation (1) and $T_e \sim 12,500$ K, we find that the ionic abundance of Mg II is $\sim 10^{-3}$. Similarly, we estimate the abundance of Si II as $\sim 10^{-3}$. At present, it is not clear if even these low cosmic abundances can be

attributed to the high ionized nebula where the C IV, N V, O III, Si IV, and S V species dominate. If, for example, the region which emits the O I, Si II, and Mg II lines has a size comparable to the radius of the primary, and a temperature of, say, ~ 8000 K appropriate for cool stellar chromospheres, its density would be $\geq 10^9 \text{ cm}^{-3}$, and the ionic abundance of Si II and Mg II would be ~ 1 . At present we cannot distinguish between these possibilities. In view of previous observations of late type giants that exhibit Mg II emission (even though these stars are not symbiotic and are not associated with a compact nebula) it remains a distinct possibility that the O I, Si II, Mg II, and Fe II? features, which have ionization potentials $\lesssim 16$ eV, arise from a cool chromosphere.

The absence of the [O II] doublet at 3726 Å and 3729 Å found by Merrill (1950) does agree with a lower estimate on density of $n_e \sim 3 \times 10^5 \text{ cm}^{-3}$ based on the maximum size of the nebula and the absence of the two-photon continuum (see § IV). Merrill (1950) observed the [O III] line at 5007 Å and [Ne III] at 3869 Å and 3967 Å. From the calculations of Kafatos and Lynch (1980) we find the intensities such that

$$I(5007 \text{ \AA})/I(3726 \text{ \AA} + 3729 \text{ \AA}) \\ \sim 100 \times N(\text{O III})/N(\text{O II}),$$

for $n_e \geq 10^6 \text{ cm}^{-3}$, where N is the relative ionic abundance. This ratio becomes $\sim 1 \times N(\text{O III})/N(\text{O II})$

for $n_e \sim 10^4 \text{ cm}^{-3}$. On the other hand,

$$\begin{aligned} I(3869 \text{ \AA})/I(3726 \text{ \AA} + 3729 \text{ \AA}) \\ \leq 1 \times N(\text{Ne III})/N(\text{O II}), \end{aligned}$$

for $n_e \lesssim 10^5 \text{ cm}^{-3}$. Assuming that $N(\text{Ne III}) \sim N(\text{O II}) \gtrsim 0.5$ and $N(\text{O II}) \leq 0.2$ (see Table 3), we conclude that n_e cannot be much less than $\sim 10^5 \text{ cm}^{-3}$.

Another estimate for the density can also be obtained from the [O III] and [Ne III] lines for which $I(5007 \text{ \AA})/I(3869 \text{ \AA}) \sim 1.5$ (Merrill 1950). Assuming again that $N(\text{Ne III}) \sim N(\text{O III})$, it follows that $n_e \geq 10^7 \text{ cm}^{-3}$ (see Kafatos and Lynch 1980). Furthermore, the observed ratio of the [O III] lines $I(4959 \text{ \AA} + 5007 \text{ \AA})/I(4363 \text{ \AA}) \sim 0.67$ (Merrill 1950) yields a value of $n_e \geq 10^8 \text{ cm}^{-3}$ for $T_e \sim 12,500 \text{ K}$ (Kafatos and Lynch 1980). From the observed strength of H α at 6563 \AA , $I(6563 \text{ \AA})/I(5007 \text{ \AA}) \sim 67$ (Merrill 1950), and for an ionic abundance of O III of ~ 0.6 (see Table 3) we find that $n_e \sim 4 \times 10^8 \text{ cm}^{-3}$. Finally, from the various ratios of the C III lines examined here we also find that $n_e \leq 10^9 \text{ cm}^{-3}$.

IV. DISCUSSION AND CONCLUSIONS

Arguments concerning the size of the nebula that envelops the RW Hya system have importance when one attempts to explain the strength of permitted and forbidden UV emission lines. The product $n_e^2 L^3$ was estimated from equation (1) and was based mainly on the continuum flux. All allowed and semiforbidden lines for densities $n \lesssim 10^9 \text{ cm}^{-3}$ are proportional to this product. Therefore, we cannot obtain an estimate for n_e or L individually from the continuum or line measurements. However, an upper limit on the nebular size can be obtained if we consider the apparent angular extent of the nebula as being $\lesssim 1''$. At 1000 pc this corresponds to $L \lesssim 1.5 \times 10^{16} \text{ cm}$ and therefore $n_e \gtrsim 3 \times 10^5 \text{ cm}^{-3}$. Lower density limits of this order are substantiated from the continuum since the distinctive broad peak centered at $\lesssim 1400 \text{ \AA}$ from the low-density H I two-photon continuum process is not seen. If the two-photon continuum was present but was essentially masked by the intense stellar continuum which we do observe at these wavelengths, we would further expect to observe greater continuum flux in the long wavelength range (2000–3200 \AA). Continuum flux measurements in the long wavelength range do not support the presence of two-photon continuum processes.

Although a precise value for the density n_e is not possible as discussed previously, we can give the general properties of the nebula $10^8 \leq n_e \leq 10^9 \text{ cm}^{-3}$, $3 \times 10^{14} \gtrsim L \gtrsim 6.5 \times 10^{13} \text{ cm}$. The chemical abundances that we have deduced are most reasonable for a nebular temperature $T_e \sim 12,500 \text{ K}$. For this reason N, O, and S are in close agreement with their expected cosmic abundances, while C and Si appear underabundant. This abundance discrepancy is possibly explained by precipitation of grains in the envelope.

Due to the uncertainties involved, n_e could be as low as 10^7 cm^{-3} , but probably not much less than this value. Densities of this order would be characteristic of chromospheric or coronal densities. It is of interest to note that for $\sim 10^9 \text{ cm}^{-3}$ the size of the nebula would only be ~ 5 times the stellar radius of the primary. Using the criterion for mass exchange between primary and secondary (Lang 1974), we find that the nebula could form entirely as a result of tidal interaction between the stars.

It would be of interest now to examine what rate of mass loss from the primary M giant is required to form the compact nebula for these high densities. If the outflowing material is moving with a velocity $\bar{v}_{\text{escape}} \sim 100 \text{ km s}^{-1}$, we find that $\dot{M} \sim 6 \times 10^{-6} M_{\odot} \text{ yr}^{-1}$ for $n_e \sim 10^8 \text{ cm}^{-3}$, $L \sim 3 \times 10^{14} \text{ cm}$; and that $\dot{M} \sim 3 \times 10^{-6} M_{\odot} \text{ yr}^{-1}$ for $n_e \sim 10^9 \text{ cm}^{-3}$ and $L \sim 6.5 \times 10^{13} \text{ cm}$. These mass loss rates are high for stars in the general region of the H-R diagram in which the primary is located. From Cassinelli (1979) we would expect values for M giants more appropriately $\dot{M} \lesssim 3 \times 10^{-7} M_{\odot} \text{ yr}^{-1}$. The high steady-state mass loss rates required to form the nebula in comparison to the values found by Cassinelli suggest that other processes are responsible for expelling material from the primary. Tidal interaction, therefore, seems a likely alternative explanation.

The X-ray luminosity arising from an accretion disk formed as a result of tidal attraction by the secondary (assuming $\lesssim 1\%$ of the nebular material falls onto the surface of the secondary) is $\sim 10^{33}$ to $10^{34} \text{ ergs s}^{-1}$ (see Novikov and Thorne 1973). Detection of soft X-ray emission in the 1–4 keV range from RW Hya would be important for determining if this high-excitation process is occurring. Observations with the Image Proportional Counter on the *HEAO B (Einstein)* satellite would prove particularly useful in this case.

We might summarize the general properties of RW Hya as follows: This symbiotic star is composed of a luminous gM2 primary and a hot subluminescent secondary identified here as a central planetary nebula star. The distance to the binary system has been estimated to be $\sim 1000 \text{ pc}$. The temperature deduced for the secondary $T_2 \sim 10^5 \text{ K}$ is such that its emission dominates the spectrum in the ultraviolet, where the cool M giant primary does not contribute significantly to the emission in this wavelength range. The relatively low excitation UV emission lines observed of O I, Si II, and Mg II may originate in the cool chromosphere ($T \lesssim 10,000 \text{ K}$) of the M giant. The high excitation and more intense lines, of which C IV (1548 \AA , 1550 \AA) is the strongest, probably originate from a compact nebula of size $L \sim 6 \times 10^{13}$ to $3 \times 10^{14} \text{ cm}$ and density $\sim 10^8$ to 10^9 cm^{-3} in which both stars are embedded. High nebular densities in this object are inferred from a general absence of significant forbidden line emission and from an apparent absence of strong H I two-photon continuum emission. Semiforbidden and allowed lines generally dominate the emission spectrum. Further work is continuing to

determine the UV time-dependent emission properties of the spectrum of RW Hya.

We acknowledge the assistance given to us by the

IUE Observatory staff during our observing sessions and for helpful discussions concerning data reduction. Additionally, we wish to thank Drs. KlingleSmith and Fahey for their assistance in reducing data.

REFERENCES

- Allen, C. W. 1973, *Astrophysical Quantities* (3d ed.; London: Athlone Press).
- Blaauw, A. 1965, in *Galactic Structure*, ed. A. Blaauw and M. Schmidt (Chicago: University of Chicago Press), p. 435.
- Boggess, A., et al. 1978, *Nature*, **275**, 1.
- Bohlin, R. C. 1975, *Ap. J.*, **200**, 402.
- Cameron, A. G. W. 1973, *Space Sci. Rev.*, **15**, 121.
- Cassinelli, J. P. 1979, *Ann. Rev. Astr. Ap.*, **17**, 275.
- Cohen, L., Feldman, U., and Doschek, G. A. 1978, *Ap. J. Suppl.*, **37**, 393.
- Edlén, B. 1972, *Solar Phys.*, **24**, 356.
- Hummer, D. G., and Mihalas, D. 1970, *M.N.R.A.S.*, **147**, 339.
- Kafatos, M., and Lynch, J. P. 1980, *Ap. J. Suppl.*, in press.
- Lang, K. R. 1974, *Astrophysical Formulae* (New York: Springer-Verlag).
- Loulergue, M., and Nussbaumer, H. 1974, *Astr. Ap.*, **34**, 63.
- . 1976, *Astr. Ap.*, **51**, 163.
- Novikov, I. D., and Thorne, K. S. 1973, in *Black Holes*, ed. C. DeWitt and B. S. DeWitt (New York: Gordon & Breach).
- Merrill, P. W. 1933, *Ap. J.*, **77**, 44.
- Merrill, P. W. 1940, *The Spectra of Long Period Variables* (Chicago: University of Chicago Press).
- . 1944, *Ap. J.*, **99**, 15.
- . 1950, *Ap. J.*, **111**, 484.
- Merrill, P. W., and Humason, M. L. 1932, *Pub. A.S.P.*, **44**, 56.
- Osterbrock, D. E. 1963, *Planet. Space Sci.*, **11**, 621.
- . 1970, *Ap. J.*, **160**, 25.
- . 1974, *Astrophysics of Gaseous Nebulae* (San Francisco: Freeman).
- Plaut, L. 1965, in *Galactic Structure*, ed. A. Blaauw and M. Schmidt (Chicago: University of Chicago Press), p. 267.
- Savage, B. D., and Mathis, J. S. 1979, *Ann. Rev. Astr. Ap.*, **17**, 73.
- Spitzer, L. 1978, *Physical Processes in the Interstellar Medium* (New York: Wiley).
- Swings, P., and Struve, O. 1941, *Ap. J.*, **94**, 291.
- . 1942, *Ap. J.*, **96**, 254.
- Wiese, W. L., Smith, M. W., and Glennon, B. M. 1966, *Atomic Transition Probabilities*, Vol. 1 (NSRDS-NBS4).
- Yamamoto, I. 1924, *Harvard Bull.*, No. 8310.

R. W. HOBBS and A. G. MICHALITSIANOS: Code 685, NASA Goddard Space Flight Center, Greenbelt, MD 20771

M. KAFATOS: Department of Physics, George Mason University, Fairfax, VA 22030